British Journal of Applied Science & Technology
3(4): 884-897, 2013

SCIENCEDOMAIN *international*
www.sciencedomain.org

Effects of Purity on the Mechanical Properties of Single-Walled Carbon Nanotubes-Polymer Nanocomposites

A. Yaya[1], D. Dodoo-Arhin[1*], B. Onwona-Agyeman[1], D.S Konadu[1], H. Mensah Brown[2] and E. Sinayobye[2]

[1]Department of Materials Science and Engineering, University of Ghana, Ghana
[2]Department of Food Process and Engineering, University of Ghana, Ghana.

Authors' contributions

This work was carried out in collaboration between all authors. Authors AY and DDA designed the study, performed the data analysis, and wrote the first draft of the manuscript. Authors BOA, DSK, HMB and ES wrote the protocol, managed the analyses of the study and literature searches. All authors read and approved the final manuscript

Research Article

Received 25th March 2013
Accepted 27th May 2013
Published 1st June 2013

ABSTRACT

This study investigated the superior mechanical properties of single-walled carbon nanotubes (SWCNTs), its polymer nanocomposites using 0.5% and 1% loading of raw and purified SWCNTs in an epoxy matrix and the degree of dispersion. The extent of load transfer between the nanotubes and the matrix was studied by analysing the second order G'-band (≈2550 cm^{-1}) of Raman Spectroscopy. The samples have been characterised from structural (Raman spectroscopy), mechanical (tensile test), physical and microstructural (SEM) point of view. Purified SWCNTs give a better reinforcing potential compared to raw SWCNTs. We found an increase in Young's Modulus (3780 MPa-4263 MPa) and toughness (62 MPa-68.8 MPa) for the nanocomposites prepared from purified SWCNTs.

Keywords: SWCNTs; Raman spectroscopy; scanning electron microscopy; epoxy; young's modulus.

**Corresponding author: E-mail: dodooa@ing.unitn.it, ayaya@ug.edu.gh;*

1. INTRODUCTION

Carbon, with its catenation potential, and the tendency to exist in different forms as graphite, graphene, fullerenes and nanotubes, makes it the most widely studied material spanning from physical to engineering sciences. Mechanical exfoliation of graphite and other methods like epitaxial growth and solvothermal synthesis yields graphene which is the building block of carbon nanotubes [1-3].

Carbon nanotubes exhibit exceptionally high modulus, high tensile strength and electrical conductivity [4,5]. This peculiar properties stems from the atomic arrangement of the graphene sheets with the sp^2 hybridized carbon-carbon bonds that roll up to form a tubular seamless structure [6]. Depending on the number of graphene sheets rolled, single walled carbon nanotube (SWCNT) can be considered as a single graphene sheet seamlessly wrapped into a cylindrical tube while multi-walled carbon nanotube (MWCNTs), as an array of concentrically arranged graphene sheets [7].

Majority of the reported mechanical properties of SWCNTs were done computationally, using methods such as molecular dynamics, ab-initio models, and empirical force constant methods. It has been shown that the mechanical properties are affected by the defect concentration, cross sectional area and method of processing the nanotubes. Values as high as 300-1470 GPa and 200 GPa have been calculated for axial Young's modulus and yield strength respectively [8-11].

The unique properties of the CNTs are attractive for a wide range of technological application. The rich chemistry of carbon also provides the opportunity to modify the structure and to optimise the property of nanotubes in structural and electrochemical applications [12,13].

SWCNTs, however when produced occur in bundles or agglomerates and in this form they have lower mechanical properties not suitable for technological applications. Dispersing the bundles to produce a composite improves the properties tremendously [14,15].

Although carbon nanotube-polymer composites offer exciting possibilities, there are still challenges to be addressed. The association of these nanotubes into bundle due to high surface energy affects the properties of nanocomposites negatively and the search for an effective way of dispersing carbon nanotubes in a polymer matrix is critical for a successful application. In addition, the higher mechanical properties of the nanotubes alone in a composite do not guarantee mechanical superior composites because the composite properties are strongly influenced by the mechanics that govern the nanotube–polymer interface; such as the degree of dispersion, the extent of load transfer and the matrix interaction with the nanotubes [16].

Different studies have shown different mechanisms of dispersing CNTs in a polymer matrix [17-27]. The differences are due to the fact that the mechanical property and the aspect ratios are usually traded for dispersion [14]. Hence, a mild and effective method of dispersion that does not destroy properties of interest is essential to utilize the exceptional properties of these materials.

Raman spectroscopy, as used in this work has historically been considered the most powerful spectroscopic technique to probe structural and electronic characteristics of carbon based materials due to their flexibility in changing their hybridization states, graphene being

the last in the long string of advances in the science of carbon [28,29]. In particular, for graphitic materials Raman spectroscopic technique provides useful information on the in-plane vibration of sp^2 carbon atoms (G band), out-of-plane stacking order (2D band), disorder (D band) [30,31], in-plane crystallite size [32], and crystallographic orientation of graphene [33].

In this work, we developed SWCNT-reinforced composites in which the as-produced SWCNTs having 20-30% impurities were purified using a series of annealing and oxidation steps described elsewhere [34]. The purified SWCNTs were later dispersed in ethanol using ultrasonic power. Nanocomposites were prepared at 0.5 and 1% of loading in an epoxy matrix. The nanocomposites showed improved mechanical property as compared to the raw epoxy matrix.

2. EXPERIMENTAL

As-prepared single wall carbon nanotubes produced by the Arc method were supplied by Carbolex with a purity of 70-80 vol% [35], average nanotube diameter of ≈ 1.4 nm. The observed impurities included ≈ 35 wt.% residual metal nickel catalyst and amorphous carbon on the outer surfaces of the bundles. The purification process was carried out by a series of oxidation and annealing [34]. The as-prepared single wall nanotubes are labelled as raw SWCNTs (r-SWCNTs) and the purified ones as p-SWCNTs.

The necessary weight fractions (0.5 wt% and 1wt %) of SWCNTs were first dispersed in ethanol using ultrasonic horn for about one hour. As the process generates enormous amount of heat, the alcohol/SWCNT mixture was placed in an ice bath during the process of sonication. Subsequently, the ethanol-nanotube mixture was mixed with the epoxy resin (E-20) which is bisphenol-F-epichlorohydrin epoxy resin with a diluent 2, 3-epoxypropyl.

The suspensions were stirred using a mini agitator (RW 16) for 12 hrs in a silicon oil bath at 60–70ºC until all ethanol was evaporated. The hardener (3-aminomethyl-3, 5, 5-trimethyl-cyclohexylamine) was then, added in the ratio of 100:30 by weight.

The nanocomposites were de-gassed in vacuum for about 20 to 25 minutes. Finally, the thick suspension was poured into a dog bone shaped silicon mould to attain a final dog bone shape.

Samples of neat epoxy (used as reference), raw-SWCNT/Epoxy composites (r-SWCNT/Epoxy) and purified-SWCNT/Epoxy composites (p-SWCNT/Epoxy) were prepared at 0.5% and 1% loading.

2.1 Characterization

Several analytical techniques were used to study the chemical and physical properties of the nanocomposites. Some of these methods are described in sections 2.1.1 to 2.1.3.

2.1.1 Tensile tests

Tensile tests of the resultant neat epoxy polymer, r-SWNT/Epoxy composite and p-SWCNT/epoxy composites each at 0.5% and 1% nanotube loading were conducted using a Zwick universal tensile testing machine (model-Z100). Each test was performed at a test

speed of 1mm/min with an extensometer attached to the sample under investigation. For each test 10 samples were examined and averaged.

2.1.2 Raman spectroscopy

Raman spectroscopy data were collected on a Renishaw 1000 micro-Raman spectrometer equipped with holographic filters to eliminate contributions from Rayleigh lines and analytical software. Samples were analysed with a 785 nm argon excitation laser (1.5 mW laser powers on the sample to avoid thermal effects) through an x50 objective lens with acquisition time of 120 s and a resolution of 2 cm^{-1} was used to focus the laser beam onto the sample surface. The dependence of the Raman peak position on the second order G' band was determined by applying tension. Static scans centred at the G' band (~2550 cm^{-1}, second-order region of the Raman spectrum) were taken with typical exposure times of 10 s and subsequently analysed. All the spectra were curve-fitted using Lorentzian / Gaussian routines, from which the G' band positions were obtained.

2.1.3 Scanning electron microscopy (SEM)

A Zeiss SEM 1540 XB Field emission gun scanning electron microscope equipped with EDS for elemental composition analysis was used for the morphological characterisation of the nanotubes and also to analyse the fracture surface of the nanocomposites.

3. RESULTS AND DISCUSSION

3.1 Dispersion Study

The dispersion and the interfacial bonding are the two important factors that control the reinforcing ability of SWCNTs in the polymer matrix. Dispersion is one of the most important parameters that influence the mechanical property of nanocomposites. For the dispersion study, SWCNTs were sonicated in ethanol (98%) for about 1 hour. The mixture was observed to be stable for several hours, which is an indication of a dispersion state. After a day, the r-SWCNTs started settling at the bottom of the container while the p-SWCNTs were still well dispersed in the mixture: an indication of a better stability than the r-SWCNTs. This stability could be attributed to the modifications made on the surface of the nanotubes whilst purifying in the oxidative environment.

The stable suspensions were dispersed again, in an epoxy matrix. For this purpose, shear dispersion was used to assimilate the nanotubes in epoxy matrix. Though, we realized a combination of sonication and shear methods work better in dispersing the nanotubes, the parameters that influence the dispersion (time, power and temperature) were not studied in this report. Nevertheless, coupling the above techniques helped to reduce the large aggregated nanotubes in to smaller agglomerates (as shown in Fig. 2 (a,b)) but in such attempt it was difficult to get individually separated SWCNTs.

Sonication of SWCNTs in ethanol improved the dispersion process, in such a way that the cavitation at the tip of the ultrasonic probe produced huge amount of shock waves that are used to overcome forces that held SWCNTs together.

During the dispersion of the nanocomposites, it was observed that, the viscosity increased and this was due to the high surface area of SWCNTs. It is also an indication of better

dispersion and interaction of SWCNTs with the epoxy matrix. On the other hand, an increase in viscosity could limit the dispersion, causing air bubbles to be trapped in the composite. These voids along with the nanotube bundles (aggregates) might act as a defect that deteriorates the mechanical properties of the composite.

3.2 Mechanical Properties

The high strength and high aspect ratio of SWCNTs can be exploited by incorporating it in a polymer matrix such as epoxy. The mechanical property of the CNT reinforced composites however depends on several factors like dispersion state, alignment of the tubes and interfacial interactions between the tubes and the matrix.

In this study, a mild dispersion method was chosen as a compromise between aspect ratio and degree of dispersion. Under high ultrasonic power and extended high shear, the tubes were observed to be degraded into graphitic network. Accordingly, the stress -strain results from the tensile tests are plotted as shown in Fig. 1a.

Generally, incorporating the raw SWCNTs into an epoxy matrix increases the Young's modulus, tensile strength and the toughness of the nanocomposites. Purifying these nanotubes further increases the Young's modulus but not the strength. For instance, the changes in Young's modulus and strength at 0.5% are plotted for the r-SWCNTs and p-SWCNTs in Fig. 1b, which clearly shows purifying the raw SWCNTs increased the Young's modulus without any increase in strength. This phenomenon has also been observed and reported for MWCNTs [35,36].

Higher increase in E-modulus was observed at 1% loading of purified SWCNTs and high tensile strength was observed at 0.5% loading of raw SWCNTs. The reason for the increase in tensile strength at 1% loading being smaller than at 0.5% loading could be due to agglomeration and re-aggregation of nanotubes leading to more defects (void) within the composite and the possibility of a failure.

Clearly, purifying nanotubes improves the Young's modulus by 3.7% and 5.7% at 0.5% and 1% loading respectively relative to the r-SWCNT/Epoxy composites.

However, no enhancement in tensile strength was observed for the p-SWCNT/Epoxy composites when compared to the r-SWCNT/Epoxy composites at similar loading of nanotubes (Table 1). The lack of improvement in tensile strength could be attributed to the shortening of tubes during purification and also, to the presence of agglomerates that might act as a defect where failure initiates.

Toughness, the amount of energy a material can absorb before rapture, can be determined from the area under the stress strain curve of a tensile test. This value has the unit of energy per volume (J/m^3). From the stress-strain curve (Fig. 1a), the area under each curve was integrated to determine the toughness, as shown in equation 1, where σ is the stress, ε is the strain and εf is the failure strain.

$$Toughness = \frac{energy}{volume} = \int_0^{\varepsilon f} \sigma d\varepsilon \quad (1)$$

The area under each curve was analysed and consequently the purified-SWCNT/epoxy and r-SWCNT/epoxy at 0.5% loading showed the highest toughness. The lower nanotube loading accompanied by increase in the toughness of the polymer matrix is attributed to the large specific surface area and high aspect ratio provided from the nanotubes which helped in increasing the toughness of the composites through crack deflection, crack pinning and crack tip blunting [38]. The reduced toughness at 1% loading compared to 0.5% loading could be due to higher rate of re-agglomeration of nanotubes capable of causing failure.

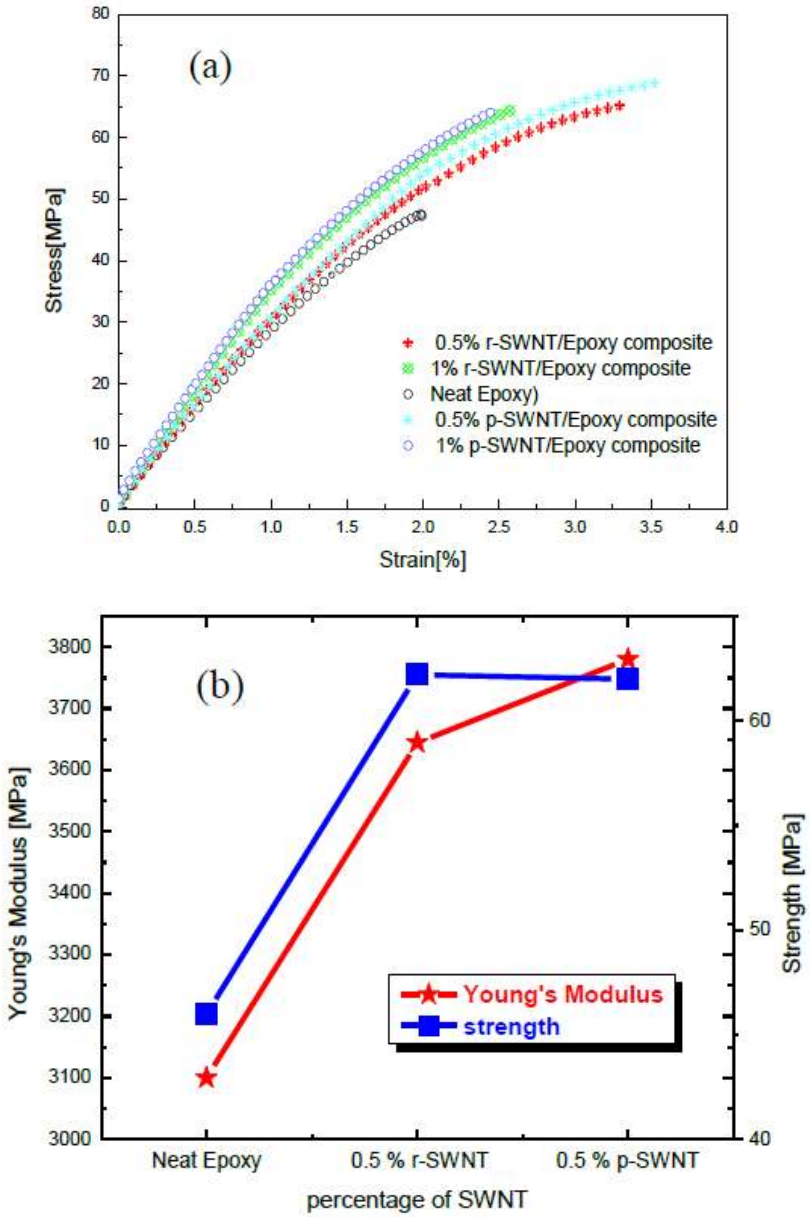

Fig. 1. (a) Stress-strain curve for neat epoxy and nanocomposites. (b) Comparison of young's modulus and strength for 0.5% loadings of raw and p-SWCNTs

Table 1. Summary of mechanical properties of the neat epoxy and nanocomposites

Sample	Young's Modulus [MPa]	Tensile Strength [MPa]
Neat Epoxy	3100	**46**
r-SWNT/Epoxy composite [0.5%]	3645	**67.5**
r-SWNT/Epoxy composite [1%]	4031	**62.2**
p-SWNT/Epoxy composite[0.5%]	3780	**68.8**
p-SWNT/Epoxy composite [1%]	4263	**62**

It is appropriate to note that some of the failures were seen to begin from a place where there were voids (air bubbles); therefore, a complete exclusion of air bubbles is necessary.

3.3 Surface Fracture Study

SWCNTs need to be de-bundled or dispersed inside a polymer matrix so that their excellent mechanical properties can be utilized. Each nanotube in the bundle is held by Van der Waals forces. Therefore, it is necessary to deliver proportional amount of force by any means to disperse the nanotubes, otherwise, only tubes that are on outer portion of the bundles could be wetted by the polymer resin. In such circumstances, the load cannot be transferred to all nanotubes due to poor interfacial strength in-between SWCNTs. The extent of dispersion and interfacial bonding between nanotubes and the epoxy matrix can be possibly studied by examining the fracture surface.

The fracture surfaces were examined after freeze-drying the nanocomposites in liquid nitrogen and investigated using SEM. The SEM investigation of the fractured raw-SWCNT/epoxy composite surface (Fig. 2a) showed SWCNTs still appear as large bundles. The presence of these bundles affects the mechanical property of the composites, as the load transfer could only occur via the outer layer of nanotubes causing slippage or pull-out between inner walls of the tubes, thereby limiting the reinforcing ability of nanotubes. The SEM micrographs of r-SWCNT/epoxy composites indicate poor wetting because the nanotubes were easily pulled out of the epoxy matrix instead of breaking, implying the lack of bonding between carbon nanotubes and epoxy.

The fracture surface of the p-SWCNT/epoxy composite (Fig. 2b) however, contained less amounts of aggregates (agglomerates) as compared to r-SWCNTs/epoxy composite (Fig. 2a). It is clear the purified nanotubes had a better adhesion with the epoxy matrix, as the tubes were seen to be wetted by the epoxy (Fig. 2b). Good wetting indicates that the polymer tends to stick to the carbon nanotube and hence it is an evidence of bonding.

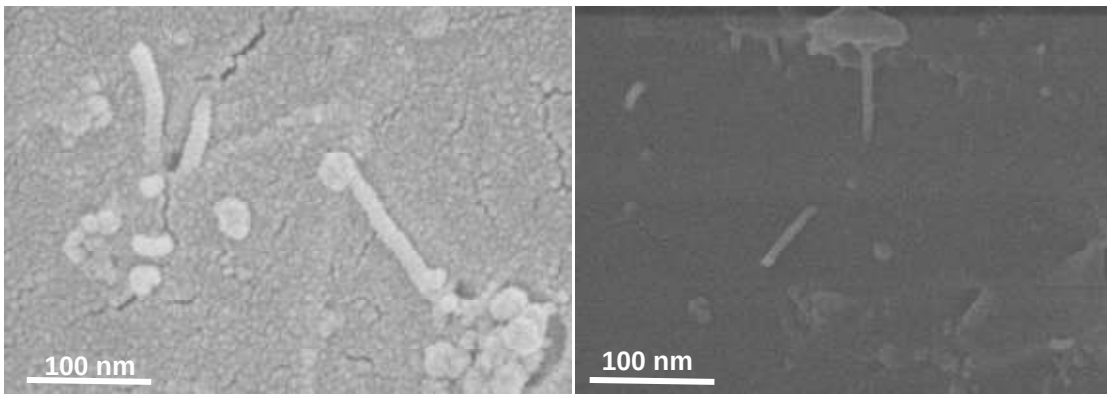

(a) (b)

Fig. 2. SEM image of fracture surface for (a) raw-SWCNTs/epoxy showing micro-aggregates with bundles of nanotubes and (b) p-SWCNTs/epoxy composites

3.4 Evaluation of Load Transfer by Raman Spectroscopy

If a strain is applied to SWCNTs, not only do their electronic and geometrical structures change but also their phonon properties. This will later influence their lattice structure, vibrational frequency and resonant intensity. These changes in electronic and phonon properties can be utilized to characterize or study how the nanotubes respond to changes in uniaxial stress [39,40].

Studies of SWCNTs under uniaxial stress by Cronin et al. [41], reported that nanotubes show a downshift of their D, G and G' Raman bands and later found that, shift of the G'-band is larger compared to other band shifts. A typical Raman spectrum for the purified SWCNTs is shown in Fig. 3.

In this study, we measured the peak shift for the sensitive second order band of single-walled carbon nanotubes observed around ~2550 cm^{-1} which has a strong peak for SWCNT. Since epoxy resin has no Raman-active vibrational mode in the vicinity of the SWCNT second order band (around 2550 cm^{-1}) that could overlap with this peak, monitoring the vibrational frequency of this second order band is convenient to examine the strain of carbon nanotubes embedded in the polymer [42]. This peak has the largest strain sensitivity causing Raman peak shift when a strain is applied.

Cooper et al. [43], also studied the second order or disorder induced G' Raman band of SWCNT reinforced epoxy matrix and reported a downshift in second order G' Raman band, which is an indication for the reinforcement of the polymer matrix by the nanotubes.

Accordingly, uniaxial strain was introduced by stretching the nanocomposites in a stretching rig attached to a computer that monitors surface strain. Static scan at ~ 2550 cm^{-1} were taken at four different places of the nanocomposites under uniaxial stress and a representative average readings were taken at that particular force (strain). Since the strain on SWCNTs is smaller than the polymer matrix, the shift rate of SWCNTs is smaller than the inherent down shift rates expected for SWCNTs.

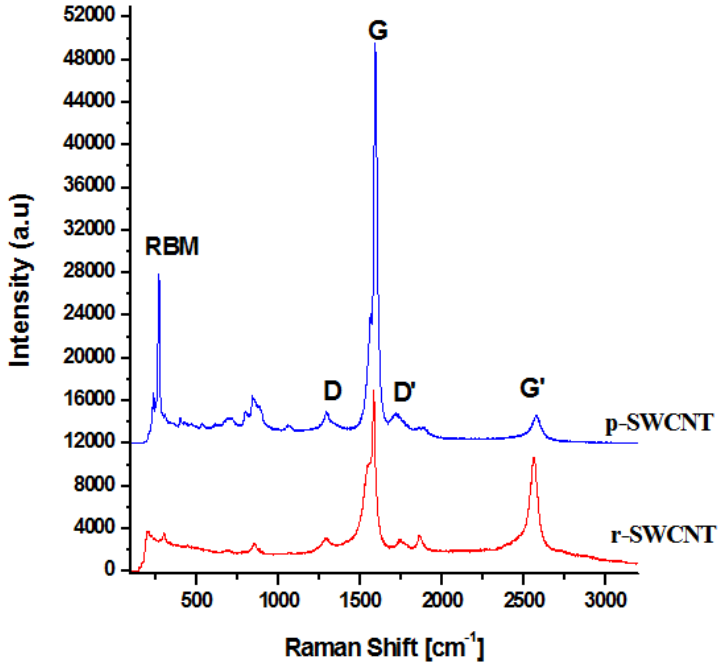

Fig. 3. Raman spectra (*785 nm Ar^+ excitation laser, resolution of 2 cm^{-1}*) for purified (p-SWCNTs) and raw (r-SWCNTs) nanotubes showing radial breathing mode (RBM), disorder mode (D), tangential mode (G) and second order tangential mode (G')

The shift in wave number of the G' band vs. the applied strain as shown in Fig. 4 (a,b), indicates that the slope trend line of the nanotubes in the 0.5% loading for the r-SWCNTs is steeper than the 1% loading of the same nanotubes: an indication of a better reinforcing potential at 0.5% loading. The poor load transfer at 1% loading of the r-SWCNTs could be attributed to the presence of relatively higher density of agglomerates and nanoparticle impurities. These agglomerates affect the load transfer in such a way that only peripheral nanotubes were bonded to the polymer and only these tubes were stressed, causing slippage of the inner tubes [44].

On the contrary, the p-SWCNT/epoxy composites showed better load transferring potential compared to the raw SWCNT/epoxy composites (Fig. 4 (c,b)).

The higher shift in wave number is an indication of a better load transfer between purified nanotubes and the epoxy matrix. Again, the high slope of the trend line at 0.5% (Fig. 4c) indicates a good reinforcement by the purified nanotube fibres; a phenomenon consistent with the aforementioned mechanical tests.

Generally, the relative increase in load carrying capacity of purified SWCNTs relative to the r-SWCNTs was due to less number of nanoparticle impurities and due to the introduction of defects on the walls of nanotubes in the process of purification which can enhance load transfer by mechanical interlocking.

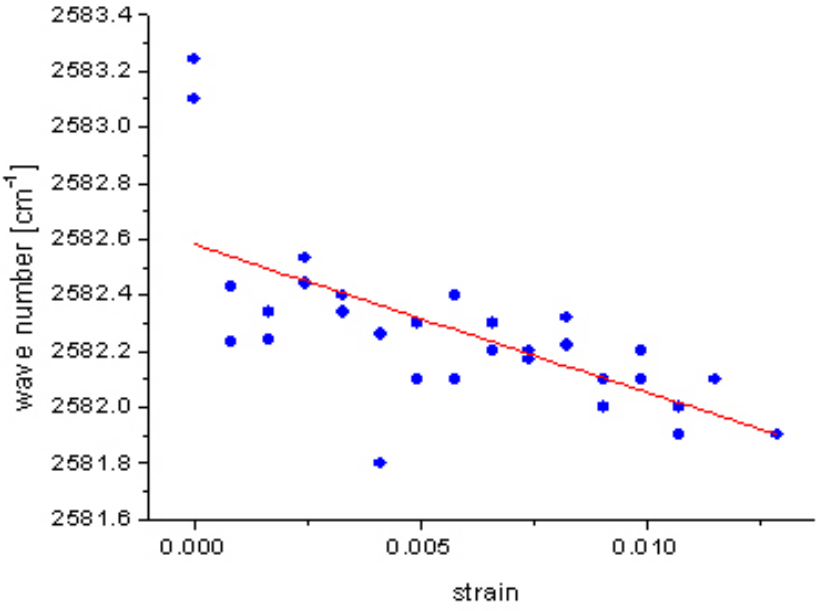
2583.4
2583.2
2583.0
2582.8
2582.6
2582.4
2582.2
2582.0
2581.8
2581.6
wave number [cm-1]
0.000
0.005
0.010
strain

(a)

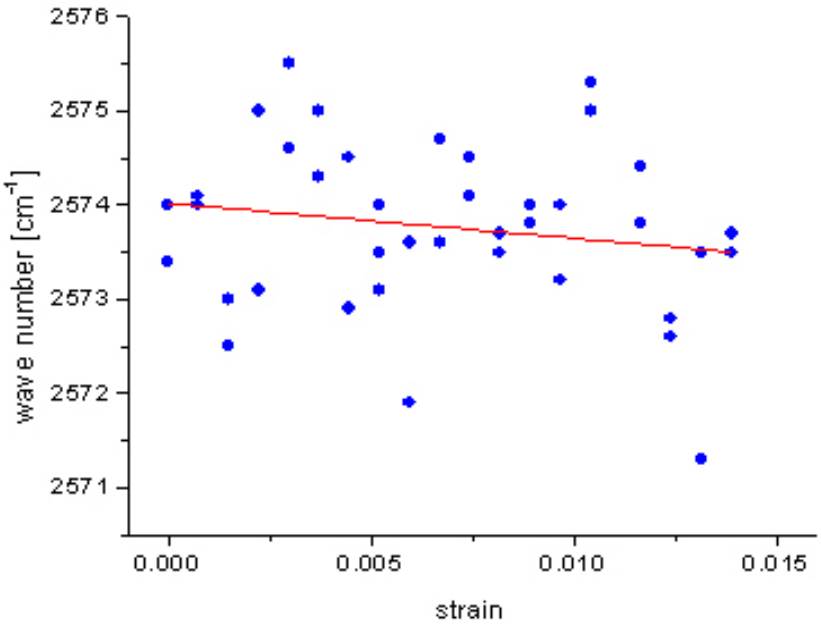
2576
2575
2574
2573
2572
2571
wave number [cm-1]
0.000
0.005
0.010
0.015
strain

(b)

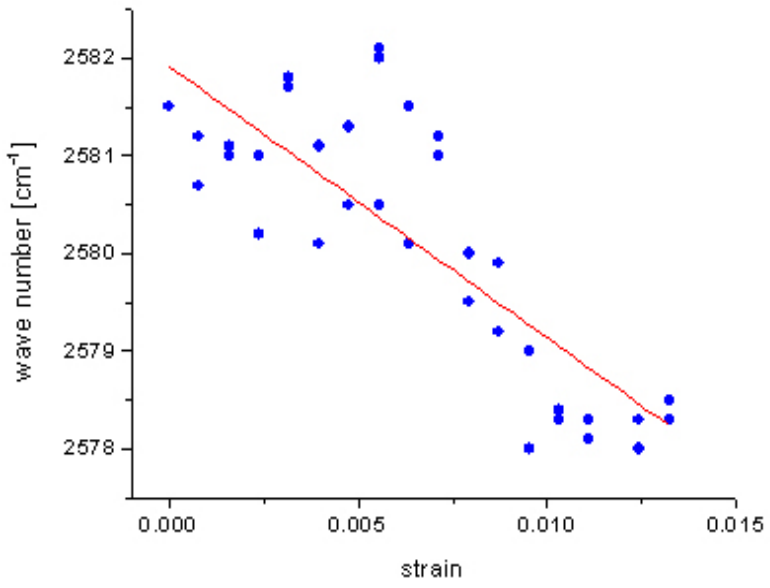

(c)

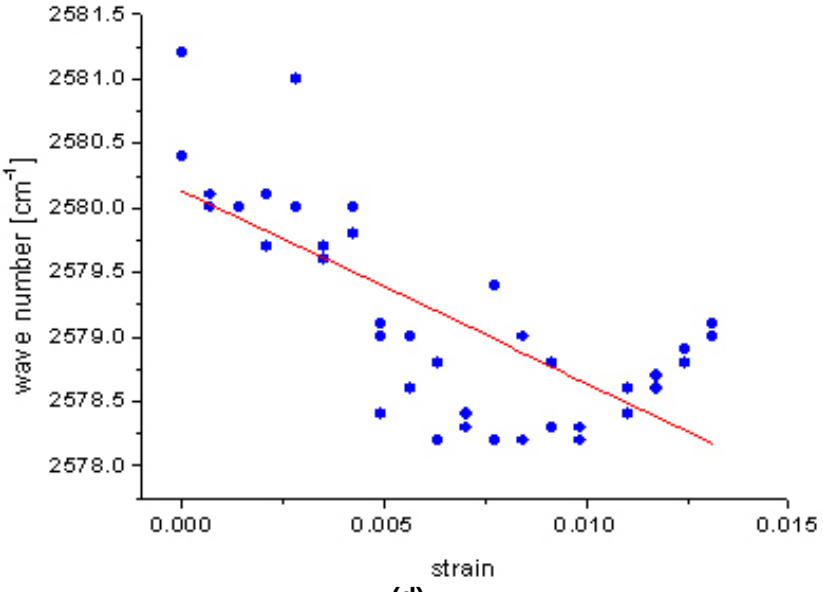

(d)

Fig. 4. Plot of wave number versus strain for Raman G'-band for raw- SWCNTs at; (a) 0.5% loading, (b) 1% loading and p-SWCNTs at; (c) 0.5% loading (d) 1% loading

4. CONCLUSION

Nanocomposites with a better mechanical property were prepared simply by purifying and excluding the nanoparticle impurities from the as-produced SWCNTs. This shows that,

impurities which come along with the nanotubes influence the property of the tubes negatively. Hence, it is important to exclude these impurities in advance before preparing nanocomposites, if possible at the manufacturing level.

Lack of uniform dispersion and poor interfacial adhesion between nanotubes and the polymer matrix are limitations that hamper full exploitations of the outstanding properties of single- walled nanotubes. Thus, it is necessary to focus on the interfacial properties between nanotubes and the matrix.

It is worth noting that, research have also shown upset reinforcement results with carbon nanotubes due weak interface as well as processing challenges [45]. However, though not the only single technique, we believe functionalizing the surface of nanotubes will significantly enhance both dispersion and adhesion.

ACKNOWLEDGEMENTS

The authors acknowledge financial support from the European Commission under the Erasmus-Mundus scheme and the University of Ghana.

COMPETING INTERESTS

Authors have declared that no competing interests exist.

REFERENCES

1. Soldano C, Mahmood A, Dujardin E. Production, properties and potential of graphene. Carbon. 2010;48(8):2127-50.
2. Hernandez Y, Lotya M, Nicolosi V, Blighe FM, Sukanta D, Duesberg G, Coleman JN. Liquid phase production of graphene by exfoliation of graphite in surfactant/water solutions. J Am Chem Soc. 2009;131(10):3611–20.
3. Choucair M, Thordarson P, Stride JA. Gram-scale production of graphene based on solvothermal synthesis and sonication. Nature Nanotechnology. 2009;4:30-33.
4. Treacy MMJ, Ebbesen W, Gibson JM. Exceptionally high Young's modulus observed for individual carbon nanotubes. Nature. 1996;381:678–80.
5. Kataura H, kumazawa Y, Maniwa Y, Umezu I, Suzuki S, Ohtsuka Y, et al. Optical properties of single wall carbon nanotubes. Synthetic metals. 1999;103:2555-58.
6. Ajayan PM, Lijima S. Smallest Carbon nanotubes. Nature. 1992;23:358.
7. Fischer JE. Carbon Nanotubes: Structure and Properties. In: Gogotsi Y, editor, nanotubes and nanofibers. Boka Raton: CRC press; 2006.
8. Ruoff RS, Lorents DC. Mechanical and thermal properties of carbon nanotubes. in: Endo M, Iijima S, Dresselhaus MS, editors. Carbon nanotubes. Great Britain-Exeter: bpc wheatons Ltd; 1996.
9. Qian D, Wagner GJ, Liu WK, Yu MF, Ruoff RS. Mechanics of carbon nanotubes. Appl Mech Rev. 2002;55:495–533.
10. Harris PJF. Carbon nanotube composites. International Materials Reviews. 2004;49:31-43.
11. Tjong SC. Structural and mechanical properties of polymer nanocomposites. Materials Science and Engineering. 2006;53:173–97.
12. Becher M, Haluska M, Hirscher M, Quintel A, Skakalov V, Dettlaff-Weglikovska U, et al. Hydrogen Storage in Carbon Nanotubes. C R Physique. 2003;4:1055–1062.

13. Saito R, Dresselhaus G, Dresselhaus MS. Physical Properties of Carbon Nanotubes. London: Imperial College Press; 1998.
14. Harris PJF. Carbon nanotube composites. International Materials Reviews. 2004;49(1):31-43.
15. Peng-Cheng M, Siddiqui NA, Marom G, Jang-Kyo K. Dispersion and functionalization of carbon nanotubes for polymer-based nanocomposites-Review. Composites Part-A. 2010;41:1345–67.
16. Desai AV, Haque MA. Mechanics of the interface for carbon nanotube - polymer composites. Thin-Walled Structures. 2005;43:1787–1803.
17. Thostenson ET, Chou TW. Processing-Structure-Multifunctional Property Relationships in Carbon Nanotube/Epoxy Composites. Carbon. 2006;44(14):2869-3148.
18. Chen H, Muthuraman H, Stokes P, Zou J, Liu X, Wang J, Huo Q, Khondaker SI et al. Dispersion of carbon nanotubes and polymer nanocomposite fabrication using trifluoroacetic acid as a co-solvent. Nanotechnology. 2007;18:415606, 1-9.
19. Thostenson ET, Tsu-Wei C. Scalable processing techniques for nanotube based polymer composites, 16th International conference on composite materials. Kyoto, Japan; 2007.
20. Chen GX, Li YJ, Shimizu H. Ultrahigh-shear processing for the preparation of polymer carbon nanocomposites. Carbon. 2007;45:2334–40.
21. Andrews R, Jacques D, Minot M, Rantell T. Fabrication of Carbon Multiwall Nanotube/Polymer Composites by Shear Mixing. Macromol Mater Eng. 2002;287:395–403.
22. Paulusse JMJ, Sijbesma RP. Ultrasound in polymer chemistry: revival of an established technique. J Polym Sci Part A Polym Chem. 2006;44:5445–53.
23. Lu KL, Lago RM, Chen YK, Green MLH, Harris PJF, Tsang SC. Mechanical damage of carbon nanotubes by ultrasound. Carbon. 1996;34:814–16.
24. Gedanken A. Sonochemistry and its application to nanochemistry. Current Science. 2003;85:1720–22.
25. Xing YC, Li L, Chusuei CC, Hull RV. Sonochemical oxidation of multiwalled carbon nanotubes. Langmuir. 2005;21:4185–90.
26. Strano M, Moore VC, Miller MK, Allen M, Haroz E, Kittrell C, et al. The role of surfactant adsorption during ultrasonication in the dispersion of single-walled carbon nanotubes. J Nanoscience and Nanotechnology. 2003;3:81–86.
27. Jinyong W, Haibin C, Yan L. Why Single-Walled Carbon Nanotubes can be dispersed in Imidazolium-based Ionic Liquids. ACS Nano. 2008;2:12, 2540-46.
28. Ferrari AC, Robertson J. Raman spectroscopy in carbons: From nanotubes to diamond. Philos Phil Trans R Soc Lond A. 2004;362:2269-2270.
29. Ferrari AC. Raman spectroscopy of graphene and graphite: Disorder, electron–phonon coupling, doping and nonadiabatic effects. Solid State Communications. 2007;143:47-57.
30. Malarda LM, Pimentaa MA, Dresselhaus G, Dresselhaus MS. Raman spectroscopy in graphene. Physics Reports. 2009;473:51-87.
31. Dresselhaus MS, Jorio A, Souza FAG, Saito R. Defect characterization in graphene and carbon nanotubes using Raman spectroscopy. Phil Trans R Soc A. 2010;368:5355-5377.
32. Cançado LG, Takai K, Enoki T, Endo M, Kim YA, et al. General equation for the determination of the crystallite size La of nanographite by Raman spectroscopy. Appl Phys Lett. 2006;88:163106.
33. Duhee Y, Young-Woo S, Hyeonsik C. Strain-Dependent Splitting of the Double-Resonance Raman Scattering Band in Graphene. PRL. 2011;106:155502.

34. Yaya A, Ewels CP, Wagner PH, Suarez-Martinez I, Gebramariam Teklay A, Rosgaard Jensen L. Purification of single-walled carbon nanotubes. Eur Phys J Appl Physics. 2011;54:10401.
35. Ci LJ, Bai JB. The reinforcement role of carbon nanotubes in epoxy composites with different matrix stiffness. Composite Science and Technology. 2006;66:599-603.
36. Bai JB. Evidence of the reinforcement role of CVD multi-walled carbon nanotubes in a polymer matrix. Carbon. 2003;41(6):1331-1334.
37. Single-Walled Nanotube General Information, retrieved on 14/03/2008 from http://www.carbolex.com/products.html.
38. Gojny FH, Wichmann MHG, Fiedler B, Schulte K. Influence of different carbon nanotubes on the mechanical property of epoxy matrix composites –A comparative study. Composites Science and Technology. 2005;65:2300-13.
39. Zhongfan L, Zhang J, Gao B. Raman spectroscopy of strained single-walled carbon nanotubes. Chem Commun. 2009;6902–18.
40. Lars Rosgaard J. Study of carbon nanotubes and carbon-polypropylene composites. Ph.D Thesis, Aalborg University; 2005.
41. Cronin SB, Swan AK, Unlu MS, Goldberg BB, Dresselhaus MS, Tinkham M. Resonant Raman spectroscopy of individual Metallic and Semiconducting single wall carbon nanotubes under uniaxial strain. Physical review B. 2005;72:035425-28.
42. Frogley MD, Zhao Q, Wagner HD. Polarized resonance Raman spectroscopy of single-wall carbon nanotubes within a polymer under strain. Physical Review B. 2002;65:113413.
43. Cooper CA, Young RJ, Halsall M. Investigation into the deformation of carbon nanotubes and their composites through the use of Raman spectroscopy. Composites Part A Applied Science and Manufacturing. 2001;32(3-4):401-11.
44. Ajayan PM, Schadler LS, Giannaris C, Rubio A. Single walled carbon nanotube-polymer composites: strength and weakness. Adv Materials. 2000;12:750-53.
45. Ci LJ, Bai JB. Novel micro/nanoscale hybrid reinforcement: multi-walled carbon nanotubes on SiC particles. Advanced Materials. 2004;16(22):2021-2024.

Peer-review history:
The peer review history for this paper can be accessed here:
http://www.sciencedomain.org/review-history.php?iid=226&id=5&aid=1440